Biophysical Journal, Volume *111*

Supplemental Information

Phasor Analysis of Local ICS Detects Heterogeneity in Size and Number of Intracellular Vesicles

Lorenzo Scipioni, Enrico Gratton, Alberto Diaspro, and Luca Lanzanò

Supporting Figures for ‘Phasor analysis of local ICS detects heterogeneity in size and number of intracellular vesicles’

L. Scipioni, E. Gratton, A. Diaspro, L. Lanzanò

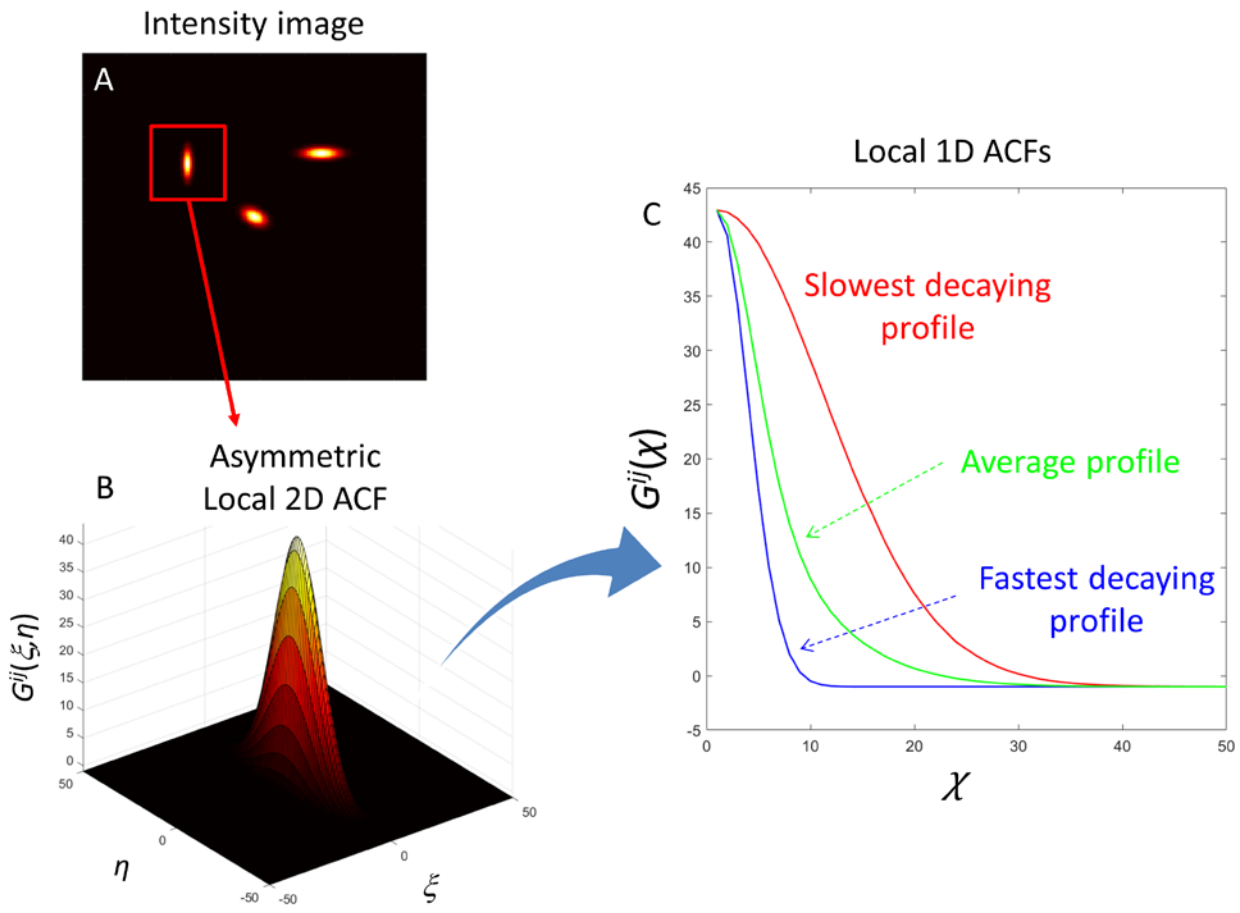

Fig.S1. Schematic representation of the PLICS algorithm in the case of asymmetric local ACFs. (A,B) Sub-image centered on an asymmetric structure (A) and corresponding asymmetric local 2D ACF (B). (C) Examples of 1D ACFs suitable for analysis: fastest decaying profile (blue), related to the thickness of the structure, slowest decaying profile (red), related to the length of the structure, and the average profile (green), obtained by averaging all angular profiles of the ACF.

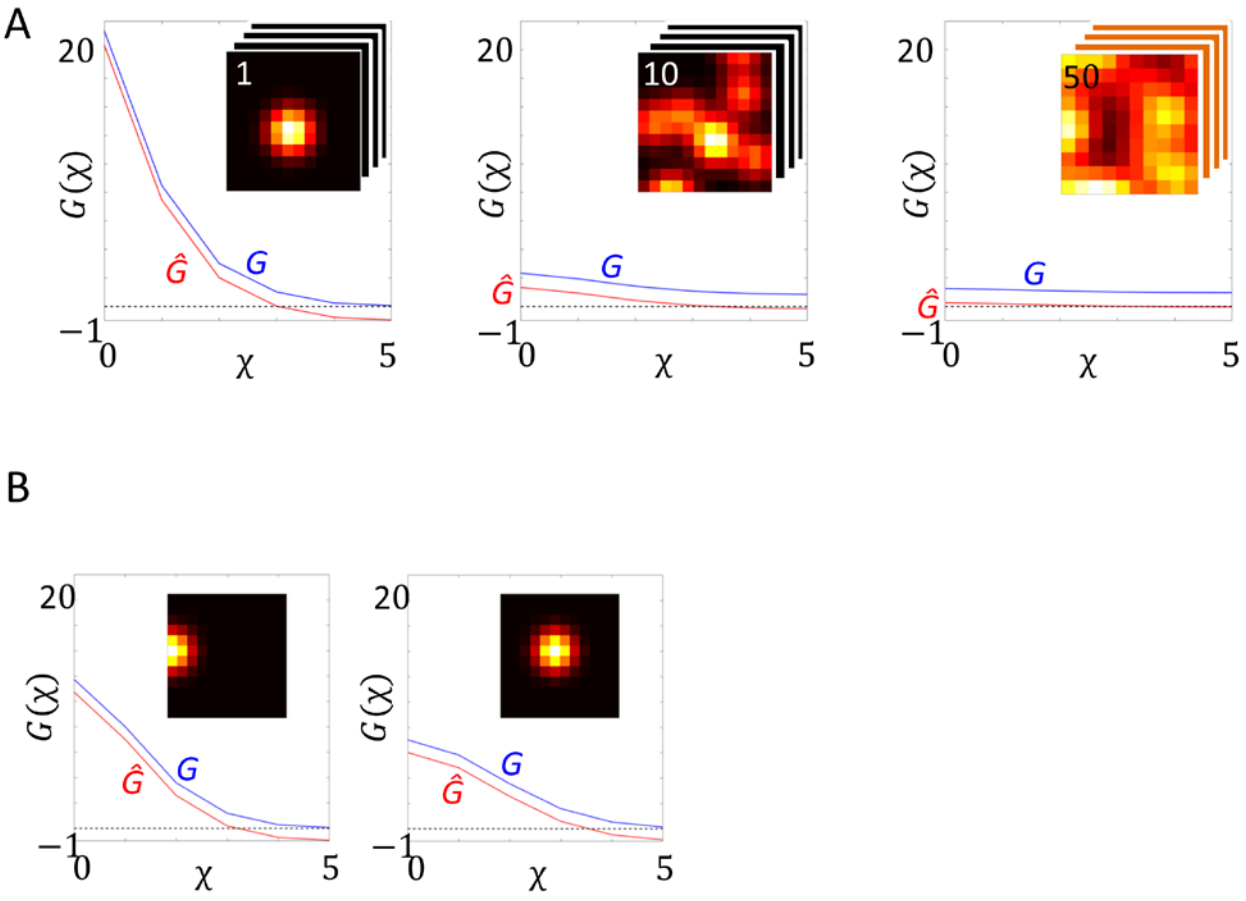

Fig.S2. (A) Average local ACF curves for N=1,10,50 (from left to right) particles (FWHM=3px) randomly distributed in a m-by-m area (m=12). The curves of $\hat{G}(\chi)$ (red) and $G(\chi)$ (blue) are obtained from the average of 1000 realizations. (B) Local ACF curves for a single particle located at the border of the sub-image (left) or close to the center (right).

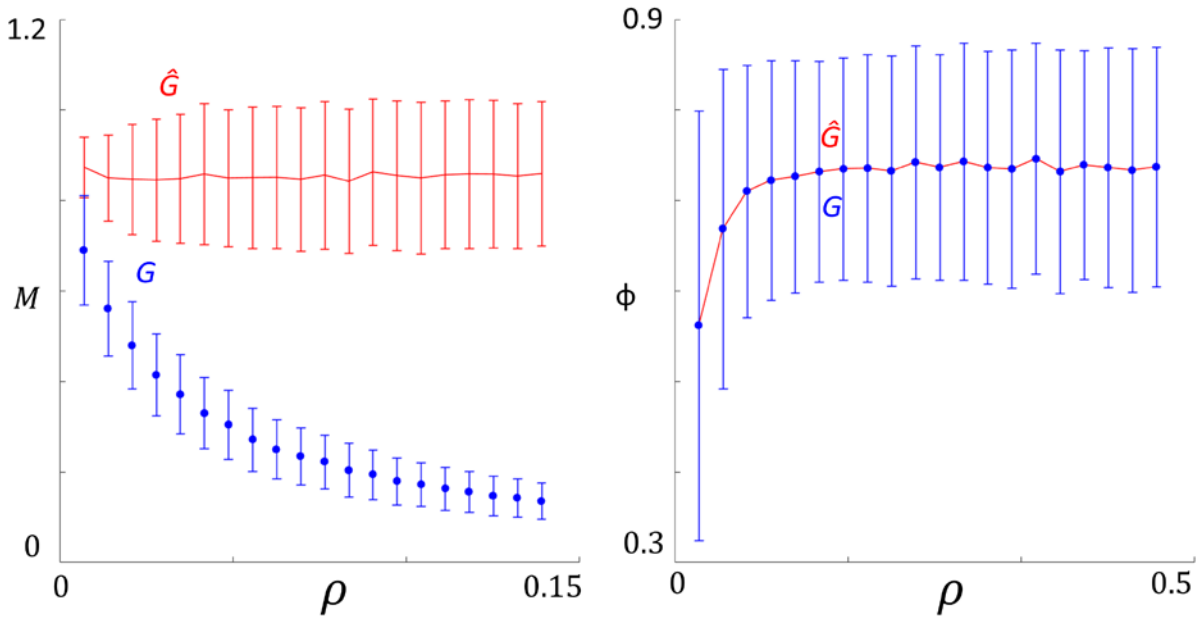

Fig.S3. Modulation (left) and phase (right) of the local correlation functions $\hat{G}(\chi)$ (red) and $G(\chi)$ (blue) (m=12) for varying particle density ρ (expressed as number of particles per pixel squared). The curves show the mean and standard deviation of 1000 simulations.

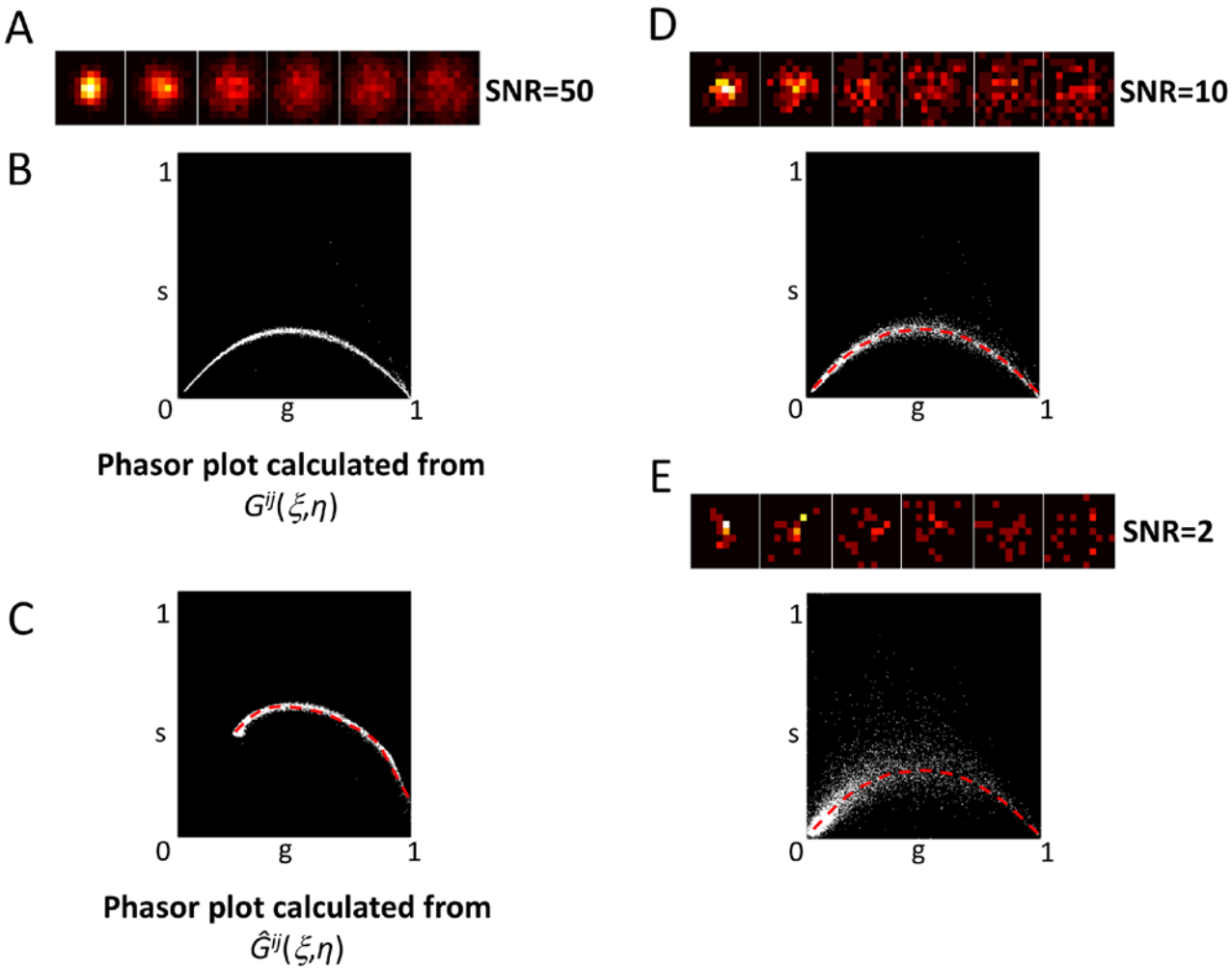

Fig.S4. (A) Series of simulated 12×12 Poisson noise affected calibration images with increasing FWHM (shown are FWHM=2,4,6,8,10 and 12 px, from left to right) and SNR=50. (B-C) Phasor plots of the correlation functions calculated on 100 repetitions for each FHWM using the $G^{ij}(\xi,\eta)$ (B) or the $\hat{G}^{ij}(\xi,\eta)$ (C) expression for the correlation function, respectively. (D,E) Same as in (A,B) but at different values of SNR, as indicated. The dashed red lines are guides to the eye.

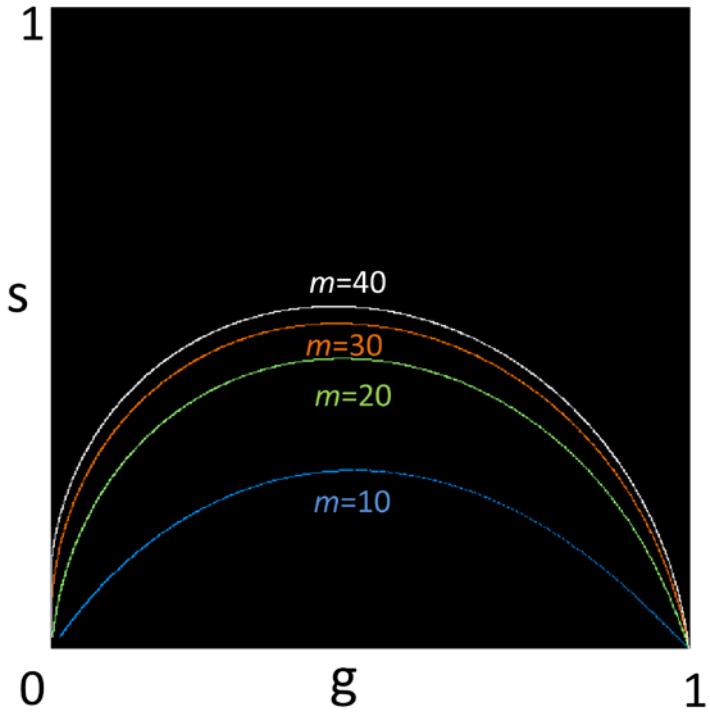

Fig.S5. Trajectories in the phasor space described by the local ACF $G(\chi)$ calculated from calibration images of increasing FWHM (from 0.1 to the width of the mask), and using different mask sizes (m=10, m=20, m=30, m=40).

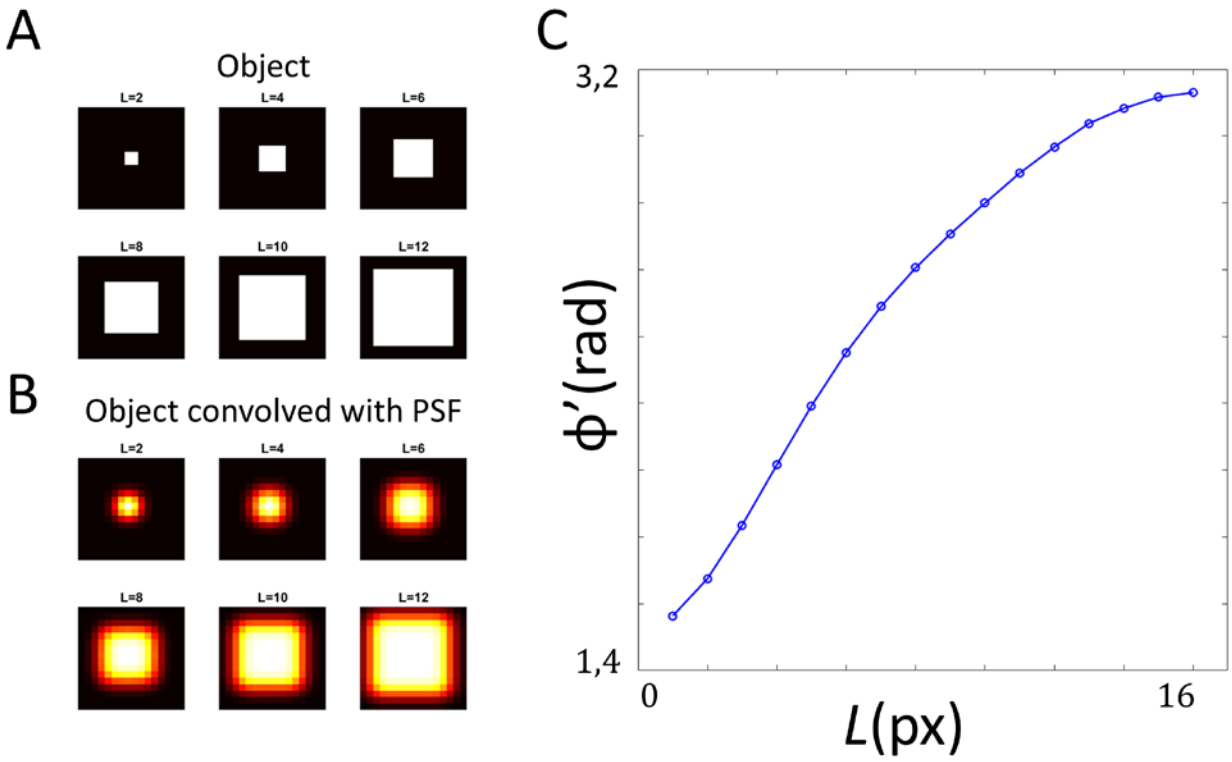

Fig.S6. Example of calibration function obtained taking into account the PSF of the microscope. (A) Simulated square objects with different lateral size (*L*=2 to 12) (B) The same objects convolved with a Gaussian PSF with FWHM=3 px. (C) Calibration curve showing the shifted phase as a function of the lateral size of the objects.

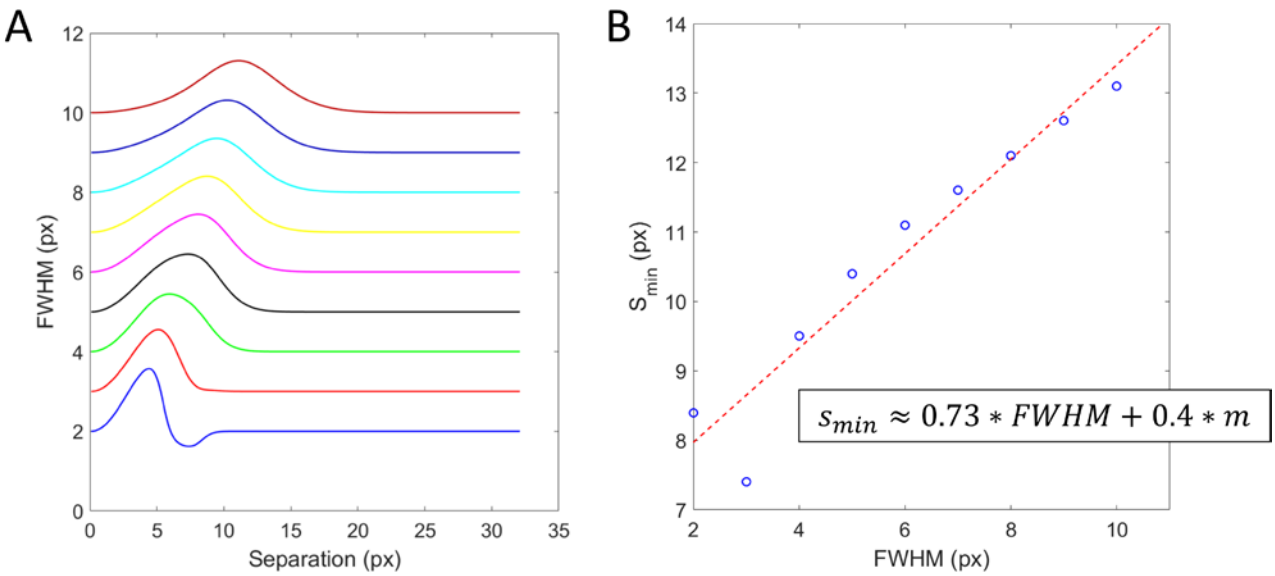

Fig.S7. (A) PLICS size as a function of the separation between two particles with FWHM ranging from 2 to 10 px, *m*=16 px. (B) Value of the separation between two particles s_{min} at which the size value deviates by 10% with respect to the correct value, plotted as a function of the FWHM (blue circles). The red dashed line is a linear fit. Shown is an approximate formula relating s_{min} to FWHM and *m*, obtained by repeating this analysis for several values of *m*.

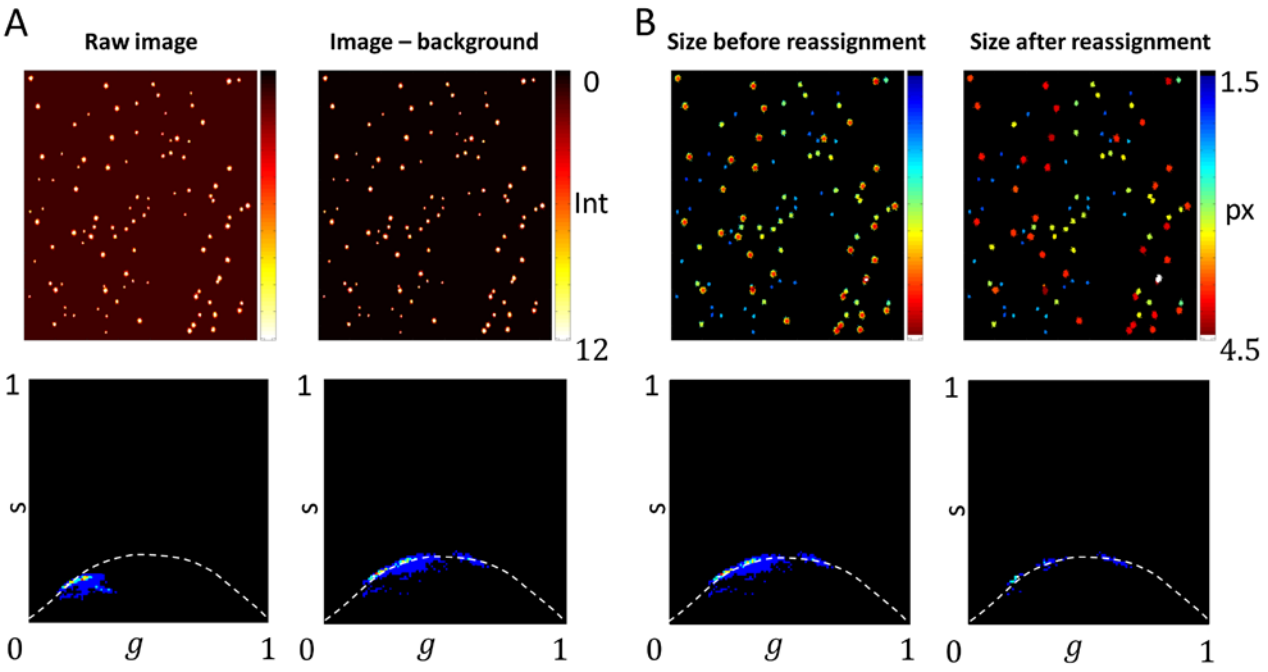

Fig.S8. Image processing in PLICS in the low density limit. (A) The first operation is a background subtraction. Without background subtraction, the phasor plot contains many points with low modulation that do not overlap with the calibration trajectory. After background subtraction, the modulation can be effectively used for determination of the size. (B) The second operation reassigns the same value of size to all the pixels belonging to the same particle. This is performed assigning to every pixel the same (*g*,*s*) coordinates computed in the brightest-intensity pixel of a circular area of diameter *m*+1 around the pixel, where *m* is the sub-image size.

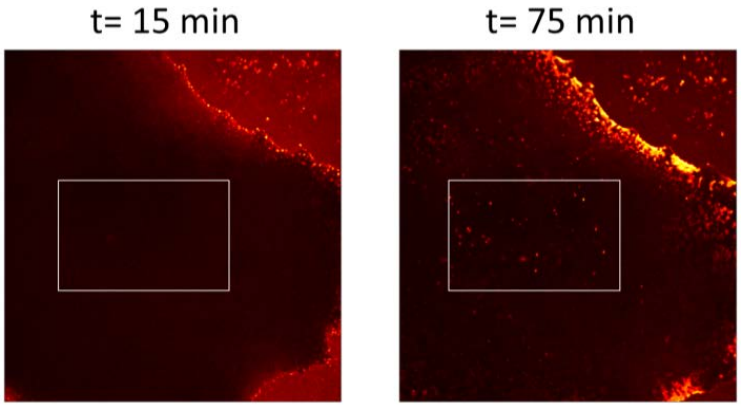

Fig.S9. HeLa cell stained at time t=0 with 10 μg/ml pHrodo Green Dextran and imaged at times t=15 min and t=75 min without any washing step. Highlighted is the rectangular ROI used for the analysis shown in Fig.7A-E. Size of the ROI is 48 μm×29 μm (181×301 px).

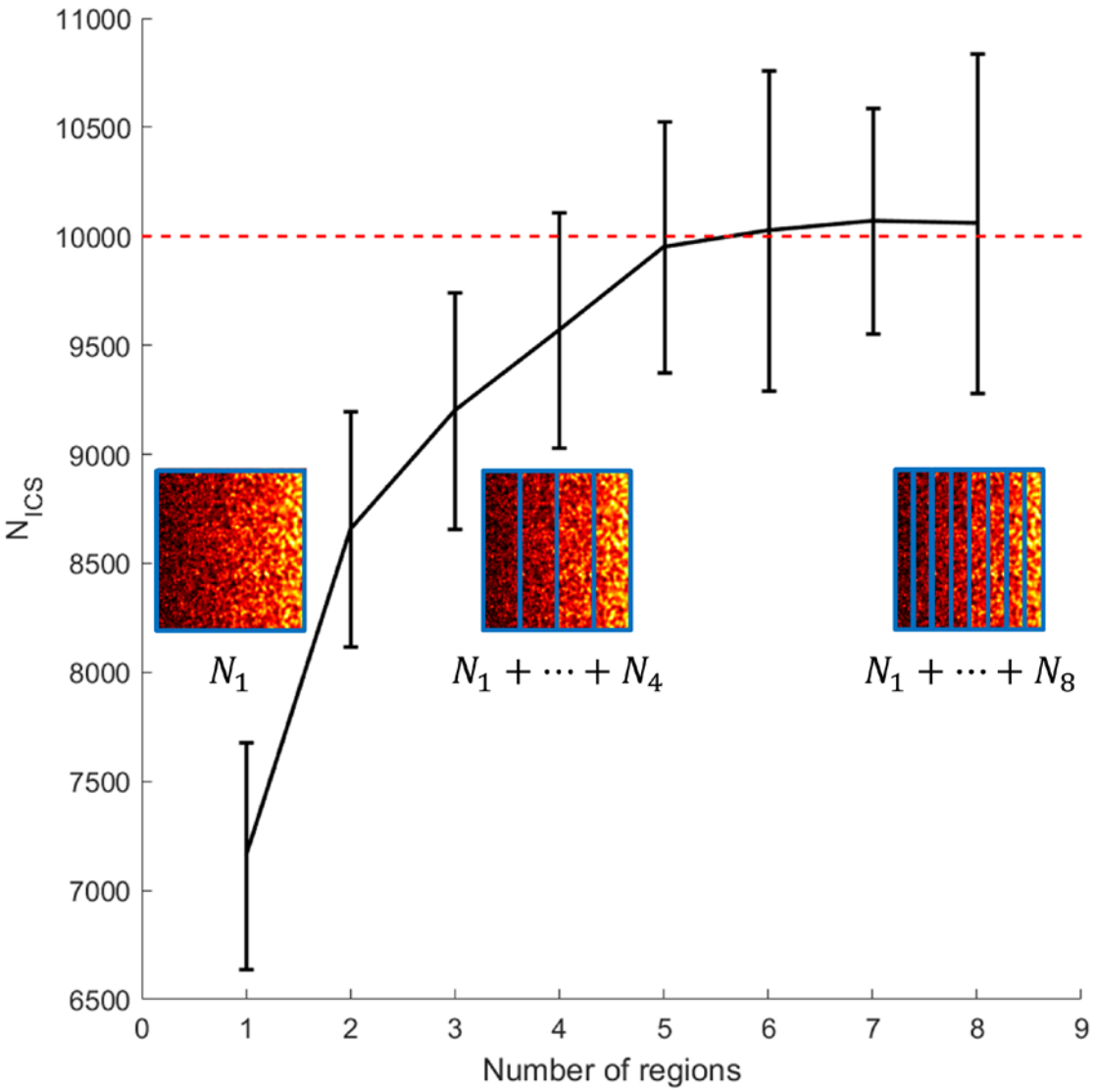

Fig.S10. Plot of the total number of particles retrieved by ICS as a function of the number of rectangular regions in which the image in Fig. 3E of the main text is segmented. The graph shows the mean and standard deviation of 100 realization. Insets shows an example of the segmentation in case of 1,4 and 8 regions.

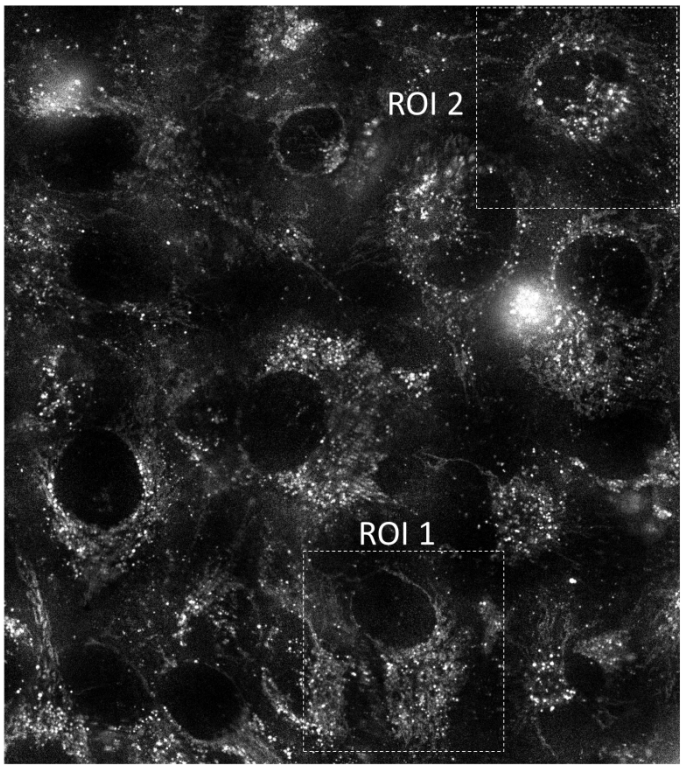

Fig.S11. Full size (1460×1640 px, pixel size=110nm) image of intracellular vesicles in confluent HeLa cells stained with pHrodo Green Dextran. Highlighted are the two ROIs selected for the analysis shown in Fig.6.

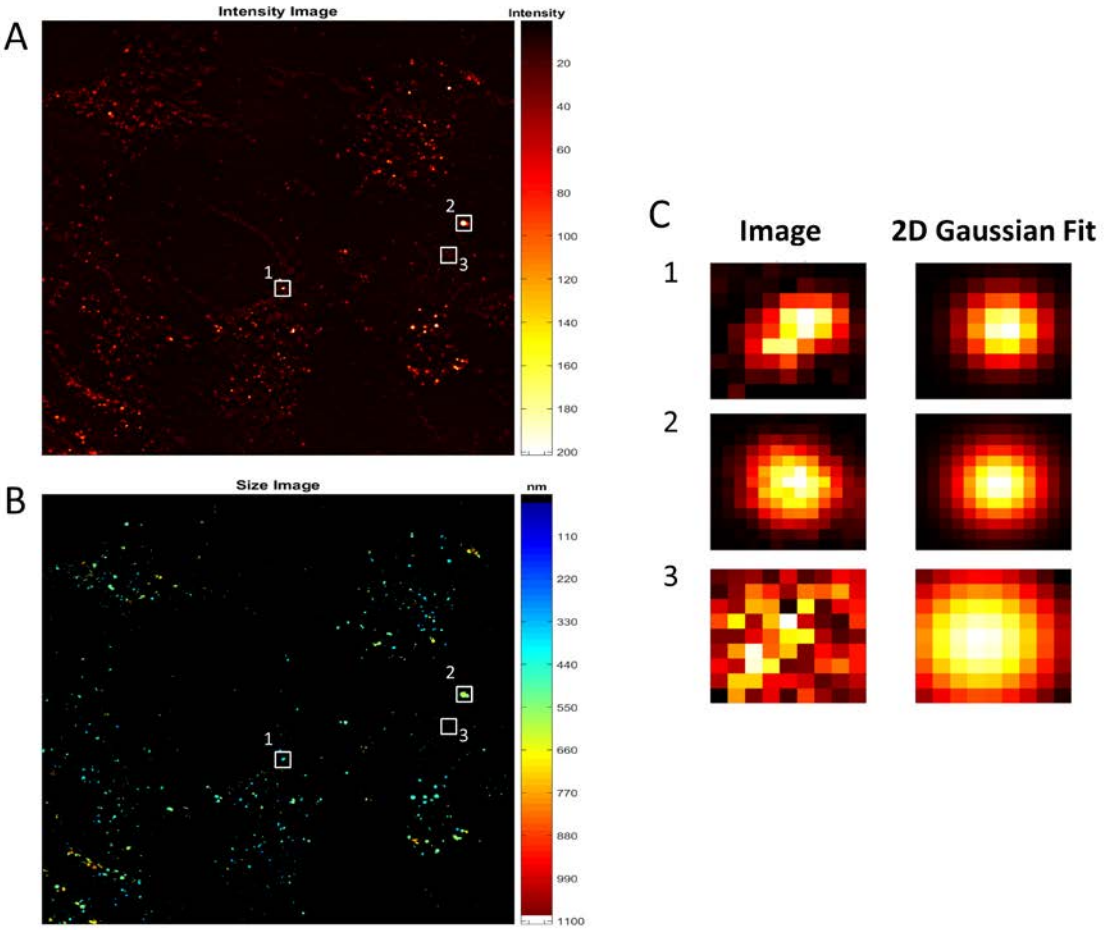

Fig.S12. Comparison between the value of size obtained from PLICS and the value of size obtained from a fitting with a 2D Gaussian function. Three ROIs are chosen as example, highlighted in the intensity (A) and size image (B). A magnification is shown (C, left column) alongside with a 2D Gaussian fitting (C, right column). The size of the structures obtained by PLICS was 405 nm (ROI 1), 622 nm (ROI 2) and 964 nm (ROI 3), respectively whereas the 2D Gaussian fitting yields 405 nm (ROI 1), 618 nm (ROI 2) and 992 nm (ROI 3), respectively. The signal-to-background ratio of the three structures is 2.45, 4.86 and 0.36, respectively.